Scintillation properties of $Bi_4Ge_3O_{12}$ down to 3 K under γ rays

M.-A. Verdier,[1,2,*] P. C. F. Di Stefano,[1,2] P. Nadeau,[1] C. Behan,[1] M. Clavel,[1] and C. Dujardin[3]

[1]*Department of Physics, Engineering Physics & Astronomy, Queen's University, Kingston, Ontario, Canada, K7L 3N6*

[2]*Université Lyon 1, Villeurbanne et CNRS/IN2P3, UMR5822, Institut de Physique Nucléaire de Lyon, Université de Lyon, Lyon, FR-69622, France*

[3]*Université Lyon 1, Villeurbanne et CNRS, UMR5620, Laboratoire de Physico-Chimie des Matériaux Luminescents, Université de Lyon, Lyon, FR-69622, France*

(Received 29 June 2011; revised manuscript received 30 November 2011; published 27 December 2011)

Bismuth germanate (BGO) has been widely used as a room-temperature scintillator in many applications for decades. Interest in it has recently increased as a low-temperature scintillator to be used in bolometers for rare-event detection. We present our time-resolved-scintillation studies of BGO down to 3 K under γ-ray excitation. Our multiple-photon-counting-coincidence-based setup allows clear identification of γ-line energies at least as low as 122 keV down to base temperature and the measurement of the light yield and decay-time constants as a function of temperature. We also discuss the time structure of the pulses and report a previously unappreciated but significant, very slow component assigned to afterglow. Finally, we demonstrate that nonlinearity of the light yield as a function of energy persists at low temperatures.

DOI: 10.1103/PhysRevB.84.214306 PACS number(s): 29.40.Mc, 78.47.jd

I. INTRODUCTION

Scintillation in solids at low temperatures has recently started to attract attention, fueled by applications in rare-event particle physics.[1–3] For instance, the ability to combine a cryogenic measurement of phonons and scintillation allows rejection of certain types of radioactive backgrounds in the search for dark-matter[4] or neutrinoless double-beta decay.[5] This technique was also used to demonstrate the instability of ^{209}Bi using a $Bi_4Ge_3O_{12}$ (BGO) scintillator.[6] Single crystals of BGO have been grown since at least 1965;[7] the crystal's high density (7.13 g/cm^3), high atomic number ($Z = 83$), and decent light output [13% of NaI(Tl) with bialkali photomultiplier tubes[8]] have ensured it is widely used at room temperature. For example, the L3 high-energy-physics experiment deployed nearly 12 000 crystals in its electromagnetic calorimeter.[9] It has also been widely studied and used for positron tomography[10] and is being considered for rare-event searches.[11] Its luminescent properties down to liquid-helium temperatures have been measured by many experiments from the middle of the 1970s to the present day,[12–18] leading to a fairly good understanding of the light emission in BGO, mainly due to the localisation of self-trapped excitons on Bi^{3+} ions. The evolution of the scintillation properties of BGO with temperature have been recently studied down to 6 K under α-particle excitation.[17] However, only a few studies have been made under γ excitation[16] because of the small amount of light obtained with a standard cryostat. Here, we relate time-resolved-scintillation studies of BGO down to 3 K under γ rays. We first describe our experimental setup and analysis method, which includes some modifications to the multiple-photon-counting-coincidence (MPCC) technique[19] and then present results for BGO in terms of the light yield (LY, the number of photons emitted for a given energy deposited) and kinetics and their evolution with temperature. We report the appearance of significant afterglow below 20 K in the samples tested. Finally, we study the nonlinearity of the LY over a range of energies and temperatures.

II. SETUP, AND ENHANCEMENTS TO THE MPCC TECHNIQUE

The multiple-photon-counting-coincidence experimental technique[19] allows a combined measurement of the LY and the decay-time structure of a scintillating crystal. For instance, it is well adapted to repeated measurements over the course of a temperature sweep. The technique includes a hardware component with a coincidence between the photodetectors triggering the digitization of photomultiplier-tube (PMT) traces. There is also an analysis component based on the identification of individual photons seen by the PMTs from a scintillation event in a crystal and a set of cuts to remove spurious events (cut on the first photon time and on the comparison between the mean arrival time of photons in a given event to the most likely mean arrival time of photons in the whole population).

The experiment we describe was carried out in two similar optical cryostats with base temperatures of 2.8 K and 3.2 K. Their compact optical geometry and good light collection[20] allow measurements with γ sources of lower energies than the α sources usually used.[19] The PMTs are secured to the outside of the cryostat on opposite sides, facing the two larger surfaces of the crystal, at room temperature, thus decoupling their response from the temperature of the cryostat. Two commercial samples of BGO, named BGO-L and BGO-Q, measuring $20 \times 10 \times 5$ mm^3, were tested, one in each cryostat. The light was detected by Hamamatsu R6095P photomultipliers adapted for photon counting and with a nominal low dark-count rate of 100 Hz. Their maximum quantum efficiency (QE) is around 400 nm, and they are well adapted for BGO, which exhibits a broad emission spectrum with a peak at 480 nm (QE $> 10\%$) at room temperature. As the emission peak shifts to 510 nm at a low temperature,[14] our PMTs are roughly 10% less efficient at detecting photons emitted at low temperatures. Standard Nuclear Instrumentation Modules (NIMs) are used to detect coincidences between the two PMTs (Fig. 1).

In the standard configuration, the excitation is provided by a ^{22}Na source, which is a β^+ emitter. The positrons are

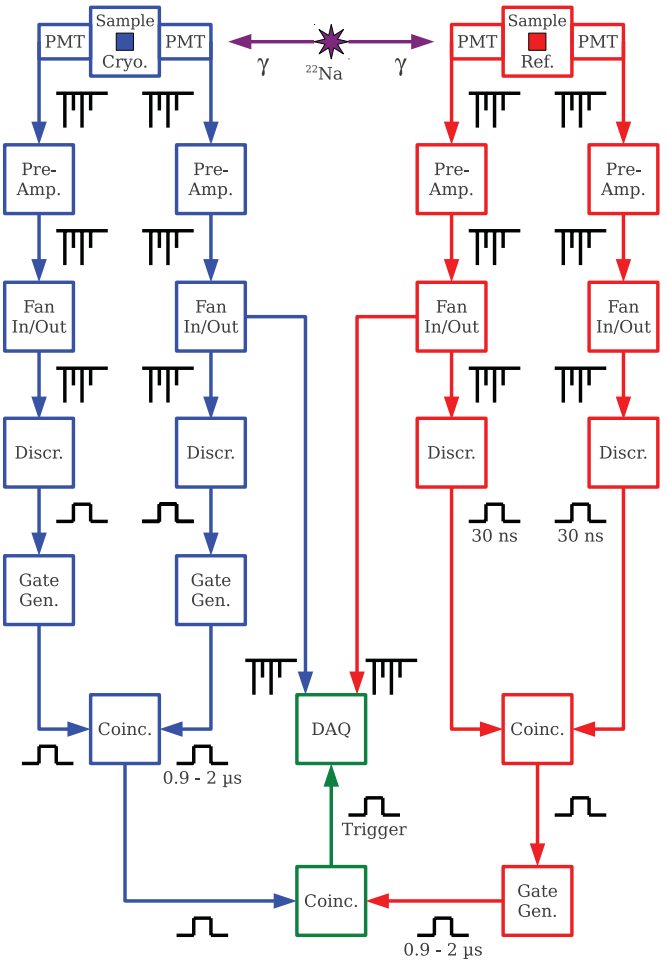

FIG. 1. (Color online) Typical setup scheme. The PMTs are well-adapted for photon counting with a low dark-count level and work in coincidence mode. The digitizer has a sampling rate of 1 GHz.

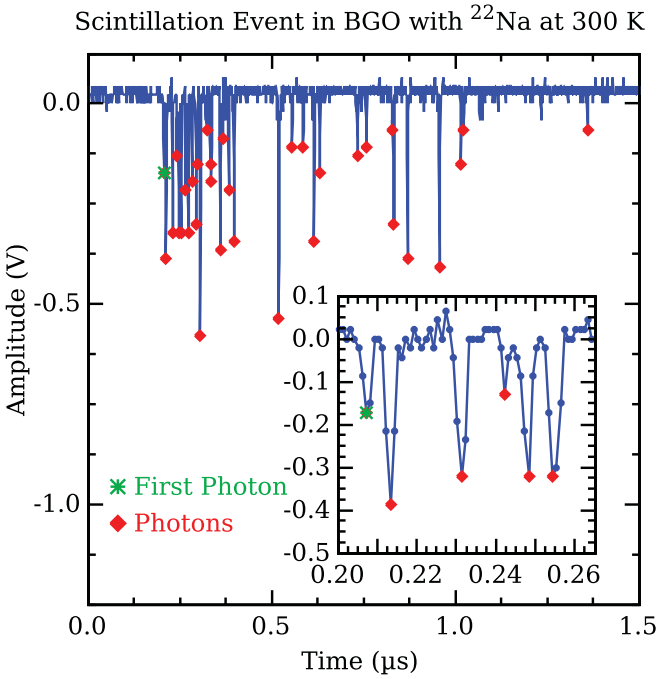

FIG. 2. (Color online) Example of a scintillation event of BGO-Q with ^{22}Na at 300 K, recorded with a sampling rate of 1 GS/s. The algorithm then recognizes the time and the amplitude of the photons (red diamonds) and in particular the first photon (green star). The inset shows a magnified view (with the same units).

annihilated by electrons in the source packaging to create two simultaneous back-to-back 511-keV γ particles. One γ particle can interact in the crystal under study in the cryostat while a second BGO crystal (set in a light-tight, room-temperature box) is used for coincidence by absorbing the second γ particle. The PMTs are in direct contact with this reference crystal, providing good light collection and allowing it to be used as a time reference for the data analysis. The measured photons are digitized by a National Instruments digitizer, working with a sampling period of 1 ns and for a duration set by the user. Only the signals coming from one of the PMTs on the cryostat and one on the reference crystal are recorded (see Fig. 1).

In order to evaluate the nonlinearity of the energy response as a function of temperature, other radioactive sources were used: ^{241}Am (60 keV), ^{57}Co (122 keV), and ^{137}Cs (662 keV). Since these sources do not supply back-to-back γ particles, the setup was simplified to a single coincidence between the two PMTs mounted on the cryostat. In this setup, the LY is calculated from the sum of photons in both PMTs. Contrary to an α source where the full energy is deposited near the surface of the crystal, a γ source creates either Compton scattering where only a fraction of the energy of the γ particle is deposited or a photoelectric absorption where all the energy is deposited. Multiple Compton scattering in the crystal can lead to a full absorption of the initial γ particle's energy, motivating the use of a larger crystal than in the previous work with α particles[17] (possibly at the expense of the energy resolution).

From the standpoint of timing, the use of PMTs with a small transit-time spread (3 ns FWHM) and a fast digitizer (1 sample per ns) allows the separation of individual photons down to ~5 ns (see Fig. 2). Moreover, in the standard MPCC technique, photon times in the average pulse shape are counted from the first photon-arrival time in each event. In the work reported here, the coincidence between the two back-to-back γ particles and the time-reference crystal provide better time resolution, allowing us to measure decay times ranging from a few tens of nanoseconds up to a few milliseconds. We note however that more precise measurements of short decay times would require the delayed-coincidence single-photon-counting technique.[19]

In both triggering modes because of the small number of photons arriving over long time scales, coincidence-window durations between 900 ns and 2 μs have been used. Moreover, when N photons arrive following an exponential distribution with a time constant τ, the distribution of the first photon follows an exponential distribution as well with a time constant of τ/N. For n time constants, the average arrival time of the first photon is given by

$$\frac{1}{\langle t_{\text{first}} \rangle} = \sum_{i=1}^{n} \frac{N_i}{\tau_i}. \tag{1}$$

From this, we estimate that the BGO reference crystal at room temperature with its very efficient light collection and short

time constants provides a timing precision better than 6 ns. This timing precision could be improved somewhat by the use of a faster room-temperature crystal (such as BaF_2, which has a fast ultraviolet component of about 600 ps[8]); however, it is unlikely that times below ∼1 ns could be reached in this setup given the typical time sampling of the digitizer.

From the standpoint of analysis, the standard MPCC cuts are applied to reject spurious events: a cut on the arrival time of the first photon in each event eliminates pretrigger pulses, and then a cut comparing the mean arrival time of photons in a particular event to a reference value from all events aids in removing pileup events. Our variation on the standard technique is to obtain the reference value by selecting the most probable average arrival time as opposed to the mean average arrival time used in the original MPCC technique, which could be slightly biased when there is a large number of pileup events. Another difference is the use of the reference time obtained with the room-temperature crystal to reconstruct pulse shapes as described above.

III. RESULTS AND DISCUSSION

Results in terms of the LY and time constants as a function of temperature are summarized in Fig. 3 and are detailed below. They evidence a main decay-time constant that accounts for the majority of photons at each temperature.

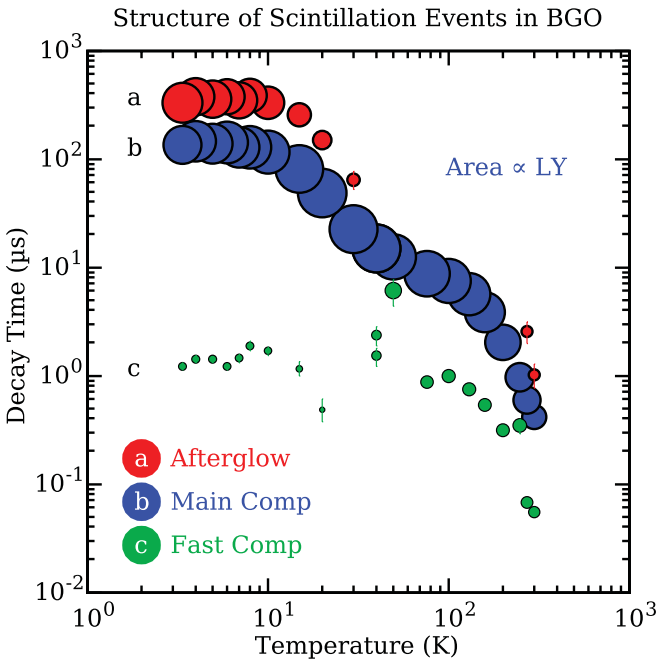

FIG. 3. (Color online) Evolution of the scintillation-decay time of BGO-Q as a function of temperature between 300 K and 3.4 K. Time constants are reported on the ordinates with vertical error bars. The LY contribution of each component is represented by the area of the circles. (b) A main contributor to the LY is identifiable. (c) A faster component only contributes a small fraction of the light. Moreover, (a) a long component, attributed to afterglow, contributes significantly below 20 K (up to ∼50% of the light below 10 K).

A. Decay time

Assuming that a scintillation event follow a series of n exponential decays with numbers of photons N_i and decay-time constants τ_i of the form

$$\frac{dN}{dt} = \sum_{i=1}^{n} \frac{N_i}{\tau_i} e^{-t/\tau_i}, \tag{2}$$

it is possible to measure the decay-time constants τ_i at each temperature by fitting the time-resolved average-scintillation event with Eq. (2). This average event is obtained by summing all of the photons from the scintillation events, taking into account their timing position with respect to the reference time. Figure 4 shows the average pulses obtained for

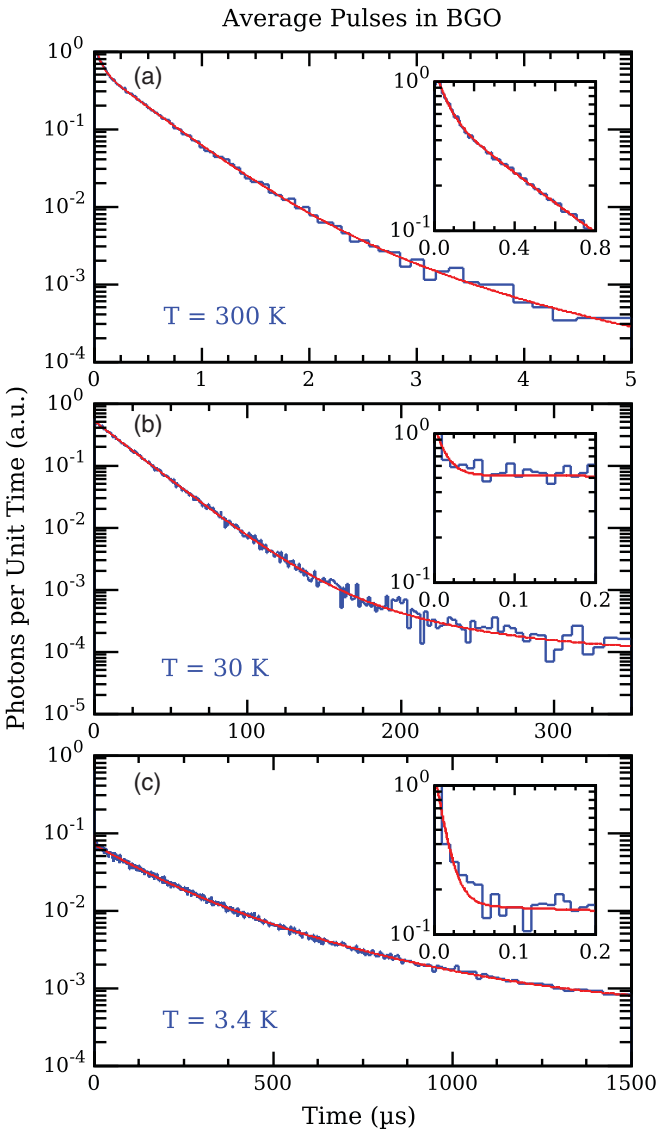

FIG. 4. (Color online) Average events of BGO-Q with ^{22}Na (511 keV for γ particles only) at temperatures of (a) 300 K, (b) 30 K, and (c) 3.4 K. The insets show magnified views (with the same units). The pulses are fitted with sums of exponentials whose numbers of components vary with the temperature. The decay-time constants obtained are: (a) 54.9 ± 4 ns, 412 ± 12 ns, 1.02 ± 0.25 μs; (b) 13 ± 6 ns, 22.6 ± 0.2 μs, 64 ± 12 μs; and (c) 12 ± 2 ns, 1.22 ± 0.09 μs, 135 ± 5 μs, 332 ± 16 μs.

TABLE I. Comparison of the LY fraction (f_{LY}) and the decay-time constant of BGO-Q and BGO-L with various experiments (Refs. 17,21, and 22). Above 6 K, only the main component (i.e., the component showing the highest fraction of light) is shown because of the different number of minor components measured in the experiments. At 6 K we also report the value of our long component, attributed to afterglow. There is good agreement between this work and MPCC results using α particles (Ref. 17) except possibly at the lowest temperatures at which previous measurements did not report afterglow.

Temperature		BGO-Q (γ)	BGO-L (γ)	Moszynski (γ)	Tsuchida (γ)	MPCC Gironnet (α)
RT(293–300 K)	f_{LY}	$79 \pm 5\%$	$76 \pm 2\%$	90%	64%	100%
	τ	420 ± 12 ns	374 ± 3 ns	300 ns	462 ± 40 ns	430 ± 8 ns
273 K	f_{LY}	$83 \pm 3\%$			90%	
	τ	598 ± 8 ns			567 ± 8 ns	
77 K	f_{LY}	$95 \pm 1\%$				95%
	τ	8702 ± 23 ns				8700 ± 100 ns
6 K	f_{LY}	$59 \pm 3\%$	$55 \pm 4\%$			
	τ	140 ± 3 μs	141 ± 5 μs			98.6%
		$40 \pm 7\%$	$44 \pm 11\%$			138 ± 0.6 μs
		375 ± 20 μs	441 ± 36 μs			

BGO-Q at 300 K, 30 K, and 3.4 K. Fits give decay-time values of 54.9 ± 4 ns, 412 ± 12 ns, and 1.02 ± 0.25 μs at 300 K; 13 ± 6 ns, 22.6 ± 0.2 μs, and 64 ± 12 μs at 30 K; and 12 ± 2 ns, 1.22 ± 0.09 μs, 135 ± 5 μs, and 332 ± 16 μs at 3.4 K. At room temperature ($\sim$300 K), we only find two decay-time constants of 55 ± 2 ns and 374 ± 3 ns for BGO-L. While cooling, the number of components varies as well as their time scales.

The main time component, coming from the luminescence of the Bi^{3+} ion,[12,17] appears clearly and increases up to 145 ± 3 μs at 3 K for BGO-L and 135 ± 5 μs for BGO-Q, i.e., an increase of a factor of about 300. Table I shows a comparison of the values of this main decay component (time constant and its fraction of the LY) with other experiments at various temperatures. Results in terms of the main time constants are broadly consistent. At the level of the secondary time components, some discrepancies appear in their number and their values between this and previous works (and indeed within previous works).

Figure 5 shows the evolution of the main decay-time constant between 300 K and 3 K for the two BGO crystals. The evolution of this main time constant with temperature follows a three-level model,[23] corrected by a nonradiative term,[24] of the form

$$\frac{1}{\tau(T)} = \frac{k_1 + k_2 e^{-D/k_B T}}{1 + e^{-D/k_B T}} + K e^{-\Delta E/k_B T}, \qquad (3)$$

where k_1 and k_2 are the radiative-decay rates from the two excited levels; K is the nonradiative-decay rate from the same levels; D and ΔE are the energy difference between the two excited states and the energy barrier for the nonradiative process, respectively; and k_B is the Boltzmann constant. The model fits our experimental data well and matches the results obtained under α particles.[17] We obtain the following parameters: $1/k_1 = 128.4 \pm 0.6$ μs, $1/k_2 = 2.58 \pm 0.01$ μs, $D/k_B = 67.7 \pm 0.1$ K, $1/K = 0.0123 \pm 0.0002$ μs, and $\Delta E/k_B = 1074 \pm 4$ K.

Concerning the two minor time constants, Fig. 3 shows that the fast one increases up to about 1 μs as the crystals are cooled. However, this component only accounts for a small fraction of the emitted light (see below). The slow component is attributed to afterglow in the crystals and may be present at higher temperatures but starts to increase greatly below 30 K, reaching about 435 ± 16 μs for BGO-L and about 332 ± 16 μs for BGO-Q. It does not appear to have been observed in previous work on BGO.[17] We propose that a higher trapping level appears with nonradiative coupling to the radiative levels. This coupling weakens as the temperature decreases, accounting for this supplementary slow time constant but preserving roughly the total emitted light. This slow component accounts for a large amount of light below 10 K (see below). Lastly, at temperatures

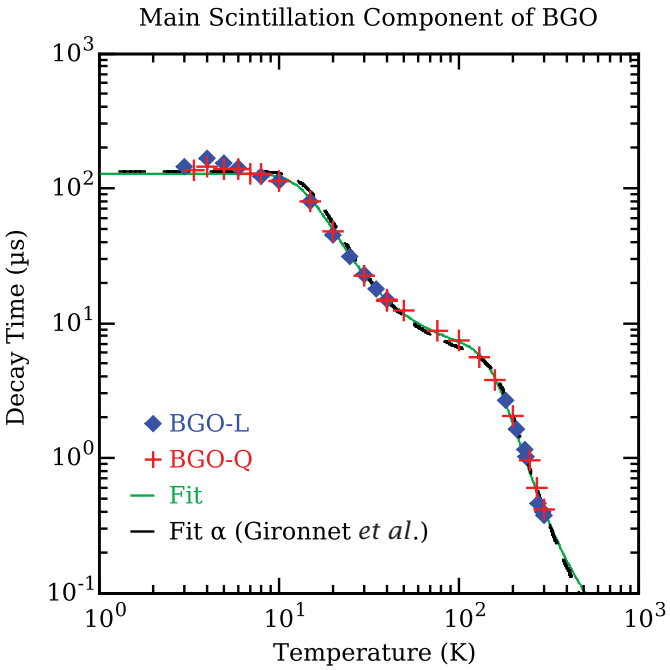

FIG. 5. (Color online) Evolution of the main decay-time constant of BGO-Q and BGO-L under γ particles between 300 K and 3 K. The combined data set has been fitted with a three-level model of Bi^{3+}. The fit curve (solid green) shows very good agreement with the result obtained under α excitation (dashed black curve) elsewhere.[17]

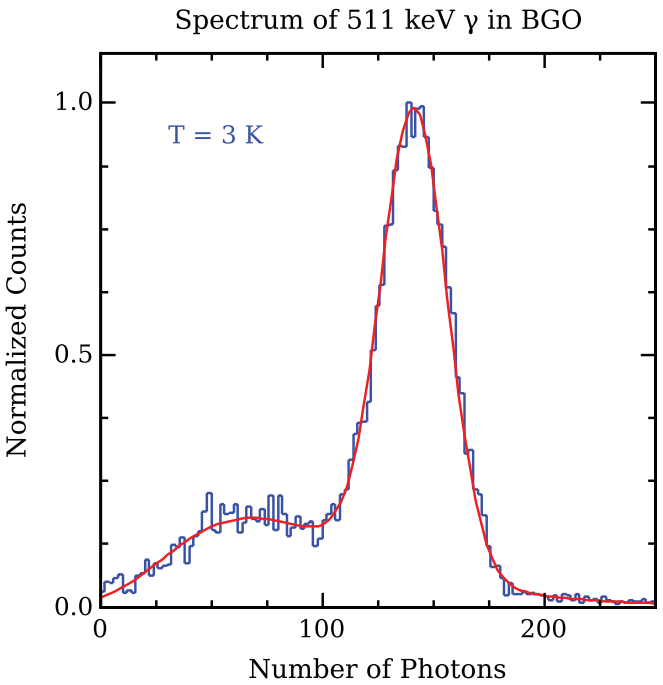

FIG. 6. (Color online) Numeric spectrum of ^{22}Na at 511 keV γ in BGO-L at 3 K. This histogram has been obtained from the number of photons counted for each individual event. The full energy peak is clearly visible with a mean value of 141.6 ± 0.2 detected photons (as fitted by a Gaussian function).

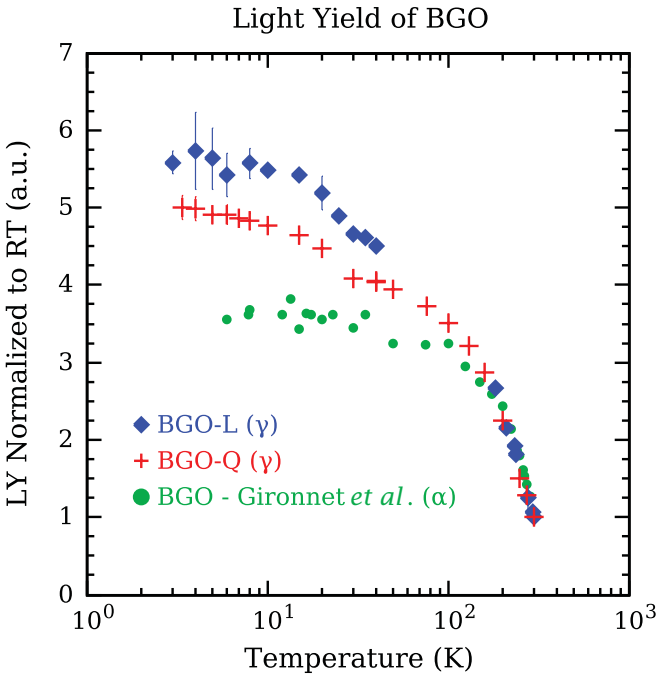

FIG. 7. (Color online) Evolution of the light yield in BGO with the temperature between 300 K and 3 K. The light yield increases by a factor of about 5.5 and 5 for the two crystals tested under γ particles in this work, noticeably more than the factor of 3.5 observed for another sample under α particles elsewhere.[17] The LY has been normalized to its room-temperature value.

below 50 K, there is an indication of a still faster time constant of about 10 ns with a negligible contribution to the LY.

B. Light yield

The position of the full-energy peak in number of photons is proportional to the LY of the crystal at all temperatures. Figure 6 shows the spectrum of BGO-L at 3 K. The full-energy peak for 511 keV is clearly visible and amounts to roughly 142 detected photons.

Because of the finite acquisition-time window, the total number of photons is underestimated, given the exponential distribution of the photons. The knowledge of the decay-time constants of each component and their relative amplitudes (N_i/τ_i) can be used to apply a correction factor to the LY, defined as

$$\mathrm{LY}_{\mathrm{corr}} = \mathrm{LY}_{\mathrm{expt}} \frac{\sum_{i=1}^{n} N_i}{\sum_{i=1}^{n} N_i (1 - e^{-t_{\mathrm{win}}/\tau_i})}, \qquad (4)$$

where t_{win} is the duration of the acquisition window. However, the effect of this correction factor is rather small on our data sets; thanks to the long acquisition times used, it is less than 10% for BGO-L and less than 1% for BGO-Q.

Figure 7 shows the evolution of the corrected LY with temperatures between 300 K and 3 K, normalized to 300 K, for the two measured crystals. The LY increases by a factor of 5.5 for one crystal and 5 for the other. The increase of the LY is higher than what has been measured under α particles for which the LY increases only by a factor of about 3.5 for the same temperature range.[17] In all cases, the LY becomes more stable below about 10 K possibly because of a reduction in the thermal quenching.

The difference in the LY evolution between the α and γ measurements is marginally compatible with the standard error of 30% quoted for the MPCC technique.[3] However, the difference could also reflect differences in the samples. Alternatively, this lower increase for α excitation can be interpreted as a variation of the quenching factor between α excitations and γ excitations, which for the same energy deposit is the ratio of the LY for each particle. Lastly, in this experiment the material regions involved are different for the two types of particles. The γ particles of 511 keV have a mean free path of roughly 1 cm in BGO and therefore interact in the bulk of the crystal whereas α particles interact only in the first few microns. The light output from α particles may be surface-quality-dependent. We speculate that the surface of the crystal contains various temperature-dependent natural traps that may affect the response to α particles but that are not present in the bulk.

The α/γ-quenching factor $Q_{\alpha/\gamma}$ has already been measured in the temperature range 253–353 K with a value of ~0.20 (Ref. 25) and with a bolometrical measurement at 20 mK with a value of ~0.17.[26] Assuming that the room-temperature-quenching factor is 0.2, an increase of the LY at 3 K by a factor of 5.5 for one crystal and 5 for the second one under γ particles and a factor of 3.5 under α particles, we find that its value at 3 K is $Q_{\alpha/\gamma} \simeq 3.5 \times 0.2/5.5 \simeq 0.13$ for BGO-L and $Q_{\alpha/\gamma} \simeq 3.5 \times 0.2/5 \simeq 0.14$ for BGO-Q. Thus, these values are lower than those previously measured; again, this could

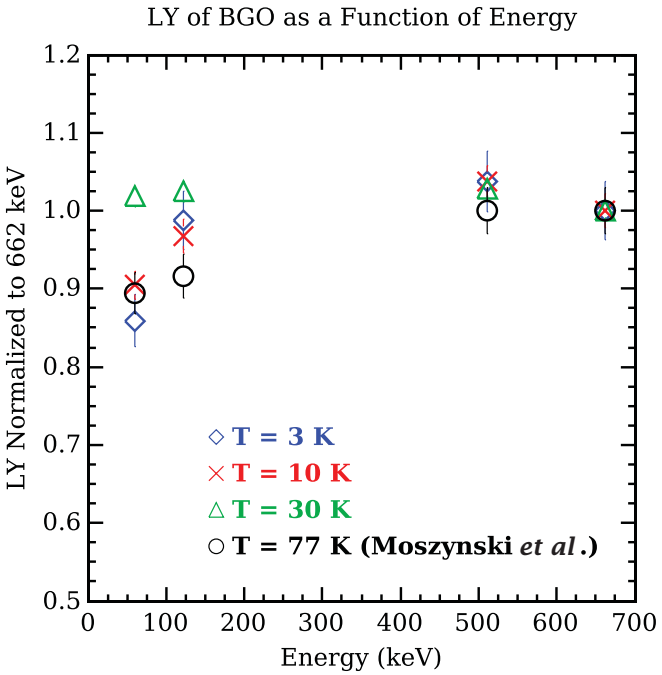

FIG. 8. (Color online) Nonlinearity of the LY of BGO-L for different temperatures. The LY is defined here as the ratio of the number of detected photons over the deposited energy. The data are normalized to 662 keV. Data at 10 K and 3 K show good agreement with the nonlinearity observed elsewhere at room temperature and 77 K (Ref. 28) though the 30-K data appear relatively linear.

also be an effect of the intrinsic quality of the different crystals measured.

By combining the independent results coming from the spectra (the LY) and the average events (the number of components and their relative contributions), one can study the quantity of light provided by each component and their evolution with temperature. Figure 3 shows that the most important part of the light comes from the main component. However, at 30 K and below, the quantity of light from this component starts to drop while the light coming from afterglow increases greatly to reach about 50% of the light at 3 K. This could be explained by the trapping level proposed previously in this work, appearing at about 30 K and leading to a transfer of excitations from the main component to the afterglow. This trapping level could moreover correspond to the thermoluminescent peak measured previously around 30 K (Ref. 15) but not seen in another study.[27] One can see also that the light coming from the fast component is negligible except around room temperature where it represents about 20% of the light.

C. Nonlinearity of the LY as a function of energy

Nonlinearity is known to occur in inorganic scintillators at low energies.[29] This phenomenon is not completely understood and has led to many measurements and theories in attempts to explain it.[28–34] Recent studies[29,32] indicate that the lower-energy shape of the LY nonlinearity can be described by the Birks equation and exciton annihilation. Indeed, this annihilation rate is proportional to the ionization density, which decreases as the deposited energy increases.

Nonlinearity has been measured in BGO at room temperature and liquid-nitrogen temperature with similar behavior in both cases.[28] We have investigated the LY as a function of energy at lower temperatures. Figure 8 shows the LY relative to that at 662 keV as a function of energy for BGO at 30 K, 10 K, and 3 K. With the exception of 30 K, we find results consistent with what has been measured at higher temperatures, thus confirming the temperature independence of the nonlinearity. However, we were unable to perform measurements at lower energies or higher temperatures because of the insufficient amount of light collected. Another study of BGO at 20 mK,[35] performed with bolometrical measurements, is compatible with a LY that is linear and, in fact, constant as a function of energy. However, the error bars on that measurement (∼40%) are in fact compatible with the nonlinearity we observe here (∼15%).

IV. CONCLUSION

This study describes the scintillation properties of BGO under γ rays down to a temperature of 3 K. Our enhanced MPCC setup enables us to measure the evolution of the light yield and the kinetics from a few tens of nanoseconds to milliseconds as a function of temperature, using tagged 511-keV γ particles. We find that the LY increases by roughly a factor of 5, noticeably more under γ excitation than under α excitation reported elsewhere, but we cannot conclude if it is an intrinsic effect in BGO or a fluctuation between samples. From the standpoint of kinetics, we confirm that the main contributor to the LY follows a three-level model, previously used to describe response to α particles and fluorescence measurements. However, we report that below 30 K a previously unobserved but significant afterglow component arises, contributing up to half of the light below 10 K. This will require extensions to the standard three-level model of kinetics, perhaps including a higher trapping level with weak nonradiative coupling to the three-level model. Finally, we provide experimental confirmation for nonlinearity of the LY as a function of energy at 4 K. This effect has yet to be confirmed by bolometric measurements of improved precision down to temperatures of tens of millikelvins.

BGO shows promise as a cryogenic scintillation-phonon detector for rare-event searches provided its radioactive background can be controlled. Despite the appearance of afterglow and the notable increase of the other decay-time constants at low temperatures, all the decay-time constants remain smaller than the typical millisecond time scales of the phonon signals and are compatible with the expected rates of the background (∼Hz) and signal ($\leqslant\mu$Hz for a dark-matter signal).

ACKNOWLEDGMENTS

This work has been funded by NSERC Canada (Grant SAPIN No. 386432) and CFI-LOF and ORF-SIF (Project No. 24536). Funding has also been provided by Agence Nationale de la Recherche (ANR) Grant SciCryo No. ANR-05-BLAN-0031. C. Behan was partially supported by NSERC USRA. We thank Y. Giraud and G. Beaulieu for computing support.

*ma.verdier@owl.phy.queensu.ca

[1] L. Gonzalez-Mestres and D. Perret-Gallix, Nucl. Instrum. Methods Phys. Res., Sect. A **279**, 382 (1989).

[2] P. C. F. Di Stefano and F. Petricca, Optical Materials **31**, 1381 (2009).

[3] V. B. Mikhailik and H. Kraus, Phys. Status Solidi B **247**, 1583 (2010).

[4] G. Angloher, C. Bucci, P. Christ, C. Cozzini, F. von Feilitzsch, D. Hauff, S. Henry, Th. Jagemann, J. Jochum, H. Kraus, B. Majorovits, J. Ninkovic, F. Petricca, W. Potzel, F. Pröbst, Y. Ramachers, M. Razeti, W. Rau, W. Seidel, M. Stark, L. Stodolsky, A. J. B. Tolhurst, W. Westphal, and H. Wulandari, Astropart. Phys. **23**, 325 (2005).

[5] L. Gironi, C. Arnaboldi, S. Capelli, O. Cremonesi, G. Pessina, S. Pirro, and M. Pavan, Opt. Mater. (Amsterdam, Neth.) **31**, 1388 (2009).

[6] P. de Marcillac, N. Coron, G. Dambier, J. Leblanc, and J.-P. Moalic, Nature (London) **422**, 876 (2003).

[7] R. Nitsche, J. Appl. Phys. **36**, 2358 (1965).

[8] G. F. Knoll, *Radiation Detection and Measurement*, 3rd ed. (Wiley, New York, 2000).

[9] R. Sumner, Nucl. Instrum. Methods Phys. Res., Sect. A **265**, 252 (1988).

[10] Z. H. Cho and M. R. Farukhi, J. Nucl. Med. **18**, 840 (1977).

[11] D. N. Grigoriev, V. F. Kazanin, G. N. Kuznetcov, I. I. Novoselov, P. Schotanus, B. M. Shavinski, S. N. Shepelev, V. N. Shlegel, and Ya. V. Vasiliev, Nucl. Instrum. Methods Phys. Res., Sect. A **663**, 999 (2010).

[12] R. Moncorgé, B. Jacquier, and G. Boulon, J. Lumin. **14**, 337 (1976).

[13] H. Piltingsrud, J. Nucl. Med. **20**, 1279 (1979).

[14] F. Rogemond, C. Pedrini, B. Moine, and G. Boulon, J. Lumin. **33**, 455 (1985).

[15] E. Dieguez, L. Arizmendi, and J. Cabrera, J. Phys. C: Solid State Phys. **18**, 4777 (1985).

[16] Z. H. Cho, M. D. Petroff, and R. Bharat, IEEE Trans. Nucl. Sci. **38**, 1786 (1991).

[17] J. Gironnet, V. B. Mikhailik, H. Kraus, P. de Marcillac, and N. Coron, Nucl. Instrum. Methods Phys. Res., Sect. A **594**, 358 (2008).

[18] M. Itoh and T. Katagiri, J. Phys. Soc. Jpn. **79**, 074717 (2010).

[19] H. Kraus, V. B. Mikhailik, and D. Wahl, Nucl. Instrum. Methods Phys. Res., Sect. A **553**, 522 (2005).

[20] M.-A. Verdier, P. C. F. Di Stefano, F. Bonte, B. Bret, M. De Jesus, G. Marot, T. Trollier, and S. Vanzetto, Rev. Sci. Instrum. **80**, 046105 (2009).

[21] M. Moszynski, C. Gresset, J. Vacher, and R. Odru, Nucl. Instrum. Methods Phys. Res. **188**, 403 (1981).

[22] N. Tsuchida, M. Ikeda, T. Kamae, and M. Kokubun, Nucl. Instrum. Methods Phys. Res., Sect. A **385**, 290 (1997).

[23] G. Beard, W. Kelly, and M. Mallory, J. Appl. Phys. **33**, 144 (1962).

[24] V. B. Mikhailik, H. Kraus, S. Henry, and A. J. B. Tolhurst, Phys. Rev. B **75**, 184308 (2007).

[25] E. Sysoeva, V. Tarasov, O. Zelenskaya, and V. Sulyga, Nucl. Instrum. Methods Phys. Res., Sect. A **414**, 274 (1998).

[26] N. Coron, G. Dambier, E. Leblanc, J. Leblanc, P. de Marcillac, and J. Moalic, Nucl. Instrum. Methods Phys. Res., Sect. A **520**, 159 (2004).

[27] W. Drozdowski, A. Wojtowicz, S. Kaczmarek, and M. Berkowski, Phys. B (Amsterdam, Neth.) **405**, 1647 (2010).

[28] M. Moszynski, M. Balcerzyk, W. Czarnacki, M. Kapusta, W. Klamra, A. Syntfeld, and M. Szawlowski, IEEE Trans. Nucl. Sci. **51**, 1074 (2004).

[29] W. Moses, S. Payne, W. Choong, G. Hull, and B. Reutter, IEEE Trans. Nucl. Sci. **55**, 1049 (2008).

[30] J. Valentine, B. Rooney, and J. Li, IEEE Trans. Nucl. Sci. **45**, 512 (1998).

[31] P. Dorenbos, J. De Haas, and C. Van Eijk, IEEE Trans. Nucl. Sci. **42**, 2190 (2002).

[32] S. Kerisit, K. Rosso, B. Cannon, F. Gao, and Y. Xie, J. Appl. Phys. **105**, 114915 (2009).

[33] G. Bizarri, W. Moses, J. Singh, A. Vasil'Ev, and R. Williams, J. Lumin. **129**, 1790 (2009).

[34] I. Khodyuk, M. Alekhin, J. de Haas, and P. Dorenbos, Nucl. Instrum. Methods Phys. Res., Sect. A **642**, 75 (2011).

[35] N. Coron, E. García, J. Gironnet, J. Leblanc, P. de Marcillac, M. Martínez, Y. Ortigoza, A. Ortiz de Solórzano, C. Pobes, J. Puimedón, T. Redon, M. L. Sarsa, L. Torres, and J. A. Villar, Opt. Mater. (Amsterdam, Neth.) **31**, 1393 (2009).